

# Edinburgh Research Explorer

# Peribiliary gland niche participates in biliary tree regeneration in mouse and in human primary sclerosing cholangitis

## Citation for published version:

Carpino, G, Nevi, L, Overi, D, Cardinale, V, Lu, W-Y, Di Matteo, S, Safarikia, S, Berloco, PB, Venere, R, Onori, P, Franchitto, A, Forbes, SJ, Alvaro, D & Gaudio, E 2019, 'Peribiliary gland niche participates in biliary tree regeneration in mouse and in human primary sclerosing cholangitis', Hepatology. https://doi.org/10.1002/hep.30871

### **Digital Object Identifier (DOI):**

10.1002/hep.30871

#### Link:

Link to publication record in Edinburgh Research Explorer

#### **Document Version:**

Peer reviewed version

# Published In:

Hepatology

# **Publisher Rights Statement:**

this is author's peer-reviewed manuscript as accepted for publication.

#### **General rights**

Copyright for the publications made accessible via the Edinburgh Research Explorer is retained by the author(s) and / or other copyright owners and it is a condition of accessing these publications that users recognise and abide by the legal requirements associated with these rights.

Take down policy
The University of Edinburgh has made every reasonable effort to ensure that Edinburgh Research Explorer content complies with UK legislation. If you believe that the public display of this file breaches copyright please contact openaccess@ed.ac.uk providing details, and we will remove access to the work immediately and investigate your claim.



DR. GUIDO CARPINO (Orcid ID : 0000-0001-8570-2519)
DR. LORENZO NEVI (Orcid ID : 0000-0003-0924-2551)
DR. DILETTA OVERI (Orcid ID : 0000-0003-3561-8903)

Article type : Original

**Title:** Peribiliary gland niche participates in biliary tree regeneration in mouse and in human primary sclerosing cholangitis

**Authors:** Guido Carpino<sup>1\*</sup>, Lorenzo Nevi<sup>2\*</sup>, Diletta Overi<sup>3^</sup>, Vincenzo Cardinale<sup>4^</sup>, Wei-Yu Lu<sup>5</sup>, Sabina Di Matteo<sup>2</sup>, Samira Safarikia<sup>2</sup>, Pasquale Bartolomeo Berloco<sup>6</sup>, Rosanna Venere<sup>2</sup>, Paolo Onori<sup>3</sup>, Antonio Franchitto<sup>3</sup>, Stuart J. Forbes<sup>5#</sup>, Domenico Alvaro<sup>2#</sup>, Eugenio Gaudio<sup>3#</sup>.

**E-mails:** guido.carpino@uniroma1.it; lorenzonevi@hotmail.it; diletta.overi@uniroma1.it; v.cardinale80@gmail.com; w.lu.3@bham.ac.uk; sabina.dimatteo@uniroma1.it; samira.safarikia@uniroma1.it; pasquale.berloco@uniroma1.it; rosanna.venere@uniroma1.it; paolo.onori@uniroma1.it; antonio.franchitto@uniroma1.it; stuart.forbes@ed.ac.uk; domenico.alvaro@uniroma1.it; eugenio.gaudio@uniroma1.it

#### Affiliations:

<sup>1</sup>Department of Movement, Human and Health Sciences, Division of Health Sciences, University of Rome "Foro Italico", Rome, 00135, Italy; <sup>2</sup>Department of Precision and Translational Medicine, Sapienza University of Rome, Rome, 00185, Italy; <sup>3</sup>Department of Anatomical, Histological, Forensic Medicine and Orthopedics Sciences, Sapienza University of Rome, Rome, 00161, Italy; <sup>4</sup>Department of Medico-

This article has been accepted for publication and undergone full peer review but has not been through the copyediting, typesetting, pagination and proofreading process, which may lead to differences between this version and the Version of Record. Please cite this article as doi: 10.1002/hep.30871

This article is protected by copyright. All rights reserved.

Surgical Sciences and Biotechnologies, Sapienza University of Rome, Latina, 04100, Italy; <sup>5</sup>Medical Research Council Centre for Regenerative Medicine, University of Edinburgh, EH16 4UU, United Kingdom; <sup>6</sup>Department of General Surgery and Organ Transplantation, Sapienza University of Rome, Rome, 00185, Italy.

\* co-first authors; ^contributed equally; #co-senior authors.

**Key words:** biliary tree stem cell, lineage tracing, WNT, Notch, cholangiopathies

# **Correspondence to:**

Prof. Guido Carpino, MD, PhD

Department of Movement, Human and Health Sciences, Division of Health Sciences, University of Rome "Foro Italico", Rome, Italy. Piazza Lauro De Bosis 6, 00135-Rome, Italy. Phone/Fax number: +39.06.36733.202. E-mail: guido.carpino@uniroma1.it

Abbreviations: IHBD: intrahepatic bile duct; EHBD: extrahepatic bile duct; PBG: Peribiliary Gland; BTSC: Biliary Tree Stem/progenitor Cell; PSC: Primary Sclerosing Cholangitis; DDC: 3,5-Diethoxycarbonyl-1,4-dihydrocollidine; wk: week; REC: recovery; PAS: Periodic Acid Schiff; SOX: Sry-related HMG box; h: human; DLL: Delta-like; PCNA: Proliferating Cell Nuclear Antigen; K: cytokeratin; AE2: anion exchanger 2; CFTR: Cystic Fibrosis Transmembrane conductance Regulator; td-Tom: td-tomato; Jag: Jagged.

Financial support: The study was supported by research project grant from Sapienza University of Rome (E.G., P.O.). The study was also supported by Consorzio Interuniversitario Trapianti d'Organo, Rome, Italy, by a sponsored research agreement (SRA) from Vesta Therapeutics (Bethesda, MD). L.N. was supported by the "Sheila Sherlock" Postdoctoral Research Fellowship programme funded by the European Association for the Study of the Liver (EASL).

**Conflict of interest:** all the authors have nothing to disclose.

# **ABSTRACT**

Mechanisms underlying the repair of extrahepatic biliary tree (EHBT) after injury have been scarcely explored. The aims of this study were to evaluate, by using a lineage tracing approach, the contribution of peribiliary gland (PBG) niche in the regeneration of EHBT after damage and to evaluate, *in vivo* and *in vitro*, the signaling pathways involved. Bile duct injury was induced by the administration of 3,5-Diethoxycarbonyl-1,4-dihydrocollidine (DDC) diet for 14 days to Krt19<sup>Cre</sup>TdTomato<sup>LSL</sup> mice. Human Biliary Tree Stem Cells (BTSC) within PBGs were isolated from extrahepatic biliary tree obtained from liver donors. Hepatic duct samples (N=10) were obtained from patients affected by Primary Sclerosing Cholangitis (PSC). Samples were analysed by histology, immunohistochemistry, western blotting, and PCR. DDC administration causes hyperplasia of PBGs and periductal fibrosis in EHBT. A PBG cell population (*Cytokeratin19'/Sox9*<sup>+</sup>) is involved in the renewal of surface epithelium in injured EHBT. The WNT signalling pathway triggers human BTSC proliferation *in vitro* and influences PBG hyperplasia *in vivo* in the DDC-mediated mouse biliary injury model. The Notch signalling pathway

activation induces BTSC differentiation *in vitro* toward mature cholangiocytes and is associated with PBG activation in the DDC model. In human PSC, inflammatory and stromal cells trigger PBG activation through the up-regulation of the WNT and Notch signalling pathways. **Conclusion:** we demonstrated the involvement of PBG cells in regenerating the injured biliary epithelium and identified the signaling pathways driving BTSC activation. These results could have relevant implications on the pathophysiology and treatment of cholangiopaties.

The biliary tree is a system of interconnected ducts comprising intrahepatic bile ducts (IHBDs) and extrahepatic bile ducts (EHBDs). Bile ducts are lined by specialized epithelial cells named cholangiocytes(1, 2). Cholangiocytes are involved in the modification of bile composition(3) and their proliferation is responsible for the turnover of the biliary epithelium(4). However, human diseases affecting the biliary tree (i.e. cholangiopathies) determine an impairment of cholangiocyte proliferative capabilities(5). In such conditions, the regeneration of interlobular bile duct epithelium is supported by hepatic stem/progenitor cells within bile ductules (6, 7). Moreover, peribiliary glands (PBGs) within large IHBDs and EHBDs contain a unique stem cell niche(8). Biliary tree stem/progenitor cells (BTSCs) in PBGs possess high self-renewal and proliferative capabilities (9, 10). However, their role in biliary regeneration has not been precisely addressed. In primary sclerosing cholangitis (PSC), which involves large IHBDs and EHBDs, cholangiocyte senescence and apoptosis are paralleled by BTSC activation followed by PBG hyperplasia in affected ducts(11). These aspects suggest a putative contribution of BTSCs in the regenerative processes involved in pathologies affecting these portions of the biliary tree when cholangiocyte proliferation is impaired.

The aims of the present study are: i) to evaluate the contribution of BTSCs in the repair of damaged EHBDs by using a mouse lineage tracing model; ii) to evaluate the signaling pathways involved in BTSC activation and differentiation both *in vitro* and *in vivo*; iii) to study the expression of activated signaling pathways within PBGs in human PSC samples.

# **MATERIALS AND METHODS**

Murine model

The animals in this study were on a C57BL6/J background. Both male and female mice were used. All animal experiments were carried out under procedural guidelines, severity protocols and with ethical permission from the University of Edinburgh Animal Welfare and Ethical Review Body (AWERB) and the Home Office (UK). The Krt19<sup>Cre</sup>TdTomato<sup>LSL</sup> mice was induced by 3 individual intraperitoneal (i.p.) injections of Tamoxifen (20mg/ml, Sigma UK) at the dose of 4mg during the light cycle. Animals received two weeks of normal diet after the last Tamoxifen injection before commencing the diet regime (T0).

To induce bile duct injury, mice were given 0.1% 3,5-Diethoxycarbonyl-1,4-dihydrocollidine (DDC) mixed with Rat & Mouse No1 Maintenance (RM1) diet (Special Diet Services), for 14 days. After DDC diet, mice were given normal chow and drinking water for the successive 14 and 28 days (recovery period). Mice were euthanized: i) after 14 days of DDC diet (DDC group: N=5), ii) after 14 days of recovery period (2-wk REC group: N=5), and iii) after 28 days of recovery period (4-wk REC group: N=5). As control, mice (N= 15) were maintained under a normal chow diet for the entire experimental period and sacrificed at the same time of mice fed with DDC diet (14, 28, 42 days after T0).

The murine extrahepatic biliary tree was dissected and fixed *en bloc*, as previously described(12).

Light microscopy, histopathology and immunohistochemistry

For immunohistochemistry, sections were incubated overnight at 4°C with primary antibodies (Supplementary Table 1). Samples were rinsed twice with PBS, incubated at room temperature with secondary biotinylated antibody and then with Streptavidin-HRP (LSAB+ System-HRP, code K0690, Dako, Glostrup, Denmark). Diaminobenzidine (Dako, Glostrup, Denmark) was used as substrate, and sections were counterstained with hematoxylin(13). For immunofluorescence, labeled isotypespecific secondary antibodies were used (AlexaFluor, Invitrogen, Life Technologies Ltd, Paisley, UK) and samples were counterstained with 4,6-diamidino-2phenylindole for visualization of cell nuclei(14). For all immunoreactions, negative controls (primary antibodies were replaced with pre-immune serum) were included. Sections were examined in a coded fashion by Leica Microsystems DM 4500 B Light and Fluorescence Microscopy (Leica Microsystems, Weltzlar, Germany), equipped with a Jenoptik Prog Res C10 Plus Videocam (Jena, Germany). Immunofluorescence stains were also analyzed by Confocal Microscopy (Leica TCS-SP2). Slides were further processed with an Image Analysis System (IAS - Delta Sistemi, Roma, Italy) and were independently evaluated by two researchers in a blind fashion.

The thickness of bile duct walls was measured by an Image Analysis System (IAS - Delta Sistemi, Rome- Italy). The extension of fibrosis was evaluated in Sirius red stains, as previously(15). The volume occupied by PGBs was expressed as the

percentage with respect to the total duct wall(8-10). For immunoreactions, the number of positive cells was automatically calculated by an algorithm on the entire section and, then, a semi-quantitative scoring system was applied (0= <5%; 1= 6– 10%; 2= 11-30%; 3= 31-50%; 4= >50%)(8). The number of Sry-related HMG box 9 (Sox9)<sup>+</sup> cells per field at 20x was calculated in six non-overlapping fields(16).

# Human tissue sourcing

Human extrahepatic biliary tree samples were obtained from the "Paride Stefanini" Department of General Surgery and Organ Transplantation, Sapienza University of Rome, Rome, Italy(17, 18). Written informed consent to use tissues for research purposes was obtained from our transplant program. All samples derived from adults between the ages of 19 and 73 years. Protocols received the approval of our Institutional Review Board, and processing was compliant with current Good Manufacturing Practice. The study protocol was conformed to the Ethical Guidelines of the 1975 Declaration of Helsinki. The research protocol was reviewed and approved by the Ethic Committees of Policlinico Umberto I of Rome, Italy. No donor organs were obtained from executed prisoners or other institutionalised individuals.

BTSC isolation, cell cultures, media and solutions

BTSCs have been isolated from human organs as previously described(9, 10). As control conditions, human (h)BTSC were cultured in a self-replication medium (i.e. Kubota's Medium: KM), as previously(9, 10). The *in vitro* effects of signalling pathway on hBTSC were evaluated by supplementing the Kubota's medium with specific Notch and WNTactivators and inhibitors. The following conditions have been tested:

- Notch pathway stimulation medium: Notch-M(19).
- WNT pathway stimulation medium: WNT-M(19).
- WNT-M + WNT inhibitor: WNT-M + Block(19).
- LPS: KM supplemented with lipopolysaccharides(20).

The exact composition of analysed conditions is furnished in supplementary materials. Cell proliferation was assessed by MTS assay, DNA Quantification (see supplementary materials), and Population Doubling Time (PDT)(20). Cell migration has been assessed by Scratch Test (21).

Quantitative reverse-transcription polymerase chain reaction (RT-qPCR) analysis

Total RNA was extracted from cell cultures by the procedures of Chomczynski and

Sacchi(22). Subsequently, the mRNA levels was analysed by RT-qPCR as

previously(17). GAPDH was used as *in vitro* reference gene. The primer sequences

are reported in **Supplementary Table 2**.

Protein extraction and Western Blot analysis

Proteins were extracted by Ripa buffer added with protease inhibitor cocktail 1:100 (SIGMA #P8340) and phosphatase inhibitor cocktail 1:100 (SIGMA #P5726). The proteins were quantized by Bradford assay using the Protein Assay Dye Reagent concentrate (Bio-Rad #500-0006). The protein extracts were resolved by SDS-PAGE on a 4-20% polyacrylamide gel (Mini-PROTEAN®TGXTM BIO-RAD #4561021) under reducing conditions and subsequently transferred on a nitrocellulose filter by 0.2 µm (BIO-RAD #1620146). Membranes were blocked overnight at 4°C with 5% Marvel skimmed milk in 1xTris Buffered Saline/Tween20 (TBST 20 mM Tris HCL, pH=8, 300mM NaCl, 0.1% Tween20) and were incubated 1h at room temperature

with primary antibody. Subsequently, membranes were rinsed with TBST and incubated for 1h at room temperature with secondary antibody peroxidase conjugated. The Light A Bolt Plus (Euroclon) Chemiluminescence System was used for detection. Used antibodies are described in **Supplementary Table 3**.

# Statistical Analysis

Data are indicated as mean±standard deviation. The Student t test or Mann–Whitney U test was used to determine differences between groups for normally- or not normally-distributed data, respectively. The Pearson correlation coefficient or the Spearman nonparametric correlation was used. A *p*-value of <0.05 was considered statistically significant. Analyses were performed using SPSS software (IBM, Milan, Italy).

#### **RESULTS**

DDC administration causes PBG hyperplasia and periductal fibrosis in the extrahepatic bile ducts

DDC mice (**Figure 1**) showed focal disruption of the surface epithelium and a marked increase of the wall area fraction occupied by PBGs (PBG area=  $15.4\pm1.9\%$ ) with respect to normal ducts ( $3.6\pm2.7\%$ , p<0.001). Two weeks after recovery from DDC injury, the surface epithelium was mostly restored and continuous without disruption. After 4 weeks of recovery, PBG area was significantly reduced ( $9.49\pm1.83\%$ ) compared to DDC mice (p<0.01). As far as mucinous cells are concerned, DDC-injured ducts presented a marked increase in the number of PAS<sup>+</sup> cells within PBGs, which returned to control value after the recovery period (histogram in **Figure 1B**).

The examination of Proliferating Cell Nuclear Antigen (PCNA) expression (a marker of proliferation, **Figure 1C**) indicated a marked increase in the number of PCNA<sup>+</sup> cells within PBGs in DDC mice ( $30.7\pm4.0\%$ ) compared to controls ( $12.7\pm2.08\%$ , p<0.01). Differently, PCNA expression by surface epithelial cells (i.e. mature cholangiocytes) did not significantly increase in DDC mice ( $9.0\pm8.5\%$ ) compared to controls ( $3.3\pm1.5\%$ ). After recovery from DDC injury, the number of proliferating PBG cells returned to control values (p<0.02 versus DDC).

Furthermore, DDC administration induced periductal fibrosis in EHBD walls (**Figure 2**); the wall thickness of EHBD walls in DDC mice was greatly increased (118.1 $\pm$ 7.1  $\mu$ m) compared to control mice (76.9 $\pm$ 15.1  $\mu$ m; p<0.01, **Figure 2A**); moreover, the extent of Sirius Red-stained fibers was increased in EHBD walls of DDC mice (0.043 $\pm$ 0.018  $\mu$ m<sup>2</sup>) compared to controls (0.0018 $\pm$ 0.0009  $\mu$ m<sup>2</sup>; p<0.01); finally, the area fraction of the duct wall occupied by Collagen I was increased in DDC mice compared to controls (**Figure 2B**). When  $\alpha$  smooth muscle actin-positive and desmin-positive myofibroblasts were counted, DDC mice showed an increase in the number of  $\alpha$  smooth muscle actin<sup>+</sup> and desmin<sup>+</sup> myofibroblasts within EHBD walls compared to controls (**Figure 2C-D**). EHBD wall thickness (r= 0.76; p<0.01) and fibrillar collagen extent (r= 0.60; p<0.05) were correlated with the PBG area.

The thickness of EHBD walls significantly reduced both after 2 and 4 weeks of recovery (108.2±4.3  $\mu$ m and 106.9±2.9  $\mu$ m; p<0.05 versus DDC mice). Sirius Red stained fiber extent and Collagen I area fraction showed a significant reduction after 4 weeks of recovery (0.017±0.009  $\mu$ m² p<0.05 compared to DDC mice). Similarly, in the recovery period, the number of  $\alpha$  smooth muscle actin<sup>+</sup> and desmin<sup>+</sup>

myofibroblasts within EHBD walls (**Figure 2C-D**) was reduced compared to DDC mice (p<0.02).

Cytokeratin(K)19<sup>-</sup>/Sox9<sup>+</sup> PBG cell population participates to the renewal of surface epithelium in injured EHBT

The expression and distribution of the stem cell marker Sox9 and mature cholangiocyte markers (K19; AE2: anion exchanger 2; CFTR: Cystic Fibrosis

Transmembrane conductance Regulator) were studied in EHBD. In controls (**Figure 3**), virtually all cholangiocytes lining surface epithelium were K19<sup>+</sup>, CFTR<sup>+</sup>, AE2<sup>+</sup> but Sox9<sup>-</sup>. Most but not all PBG cells expressed K19, and the percentage of K19<sup>-</sup> cells accounted for nearly 5%. Rare PBG cells expressed AE2 and CFTR. PBG contained Sox9<sup>+</sup> cells that accounted for nearly 10% (8.7±3.2%); a Sox9<sup>+</sup> PBG cell subpopulation was K19<sup>-</sup> and located at the bottom of PBGs.

In DDC mice (**Figure 3**), the percentage of Sox9 $^+$  cells increased both in PBGs (48.0 $\pm$ 5.6%) and in surface epithelium (15.3 $\pm$ 6.3%) compared to controls (p<0.05); interestingly, surface epithelial cells in DDC mice were K19 $^+$  but almost all negative for CFTR and AE2.

To investigate the possible role of K19<sup>-</sup>/Sox9<sup>+</sup> PBG cell population in the renewal of surface epithelium and mature cholangiocyte turnover, we analyzed a lineage tracing system in the DDC model. To label cells we used the Krt19CreER<sup>T</sup>LSL<sup>tdTomato</sup> mouse and found labelling (td-Tom positivity) strictly specific to the epithelial cells within the EHBD. In controls (**Figure 4**), the percentage of td-Tomato negative (td-Tom<sup>-</sup>) cells in the surface epithelium was low (5.4±2.9%) and td-Tom<sup>+</sup> cells lining EHBDs

represented >90% of cells; cholangiocytes lining EHBD in normal conditions were constantly K19<sup>+</sup> and Sox9<sup>-</sup>, as demonstrated in **Figure 3**. These observations confirmed that the slow physiological turnover of biliary epithelium was achieved by the proliferation of mature K19<sup>+</sup> cholangiocytes. In DDC mice (**Figure 4A**), the number of K19<sup>+</sup>/td-Tom<sup>-</sup> cells within the surface epithelium greatly increased to 34±8.21% (*p*<0.001 versus controls). In DDC mice, some td-Tom<sup>-</sup> cells within surface epithelium were Sox9 positive (**Figure 4C**); contrarily, these cells were AE2/CFTR negative, given the demonstrated lack of AE2/CFTR expression in surface epithelium of DDC mice (**Figure 3**).

During recovery phase, the percentage of td-Tom<sup>-</sup> cells within the surface epithelium progressively decreased at 2 and 4 weeks (p<0.05 versus DDC mice) but remained significantly higher compared to controls (p<0.05; **Figure 4B**). td-Tom<sup>-</sup> cells within surface epithelium progressively showed phenotypic features of mature cholangiocyte differentiation, such as the loss of Sox9 positivity at 2 weeks (not shown) and the appearance of CFTR expression at 4 weeks (**Figure 4D**).

WNT pathway triggers human BTSC proliferation in vitro and influences PBG hyperplasia in DDC-mediated duct injury in mice.

The *in vitro* administration of R-spondin 1 (WNT activator) significantly increased BTSC proliferation as demonstrated by MTS assay, population doubling time, DNA concentration, Cyclin D1 expression, and *PCNA* gene expression (**Figure 5A and Supplementary Figure 1**); R-spondin 1 also increased cell migration as demonstrated by the scratch test (**Supplementary Figure 1**). The administration of a WNT inhibitor prevented these effects. Interestingly, R-spondin 1 administration did

not change the expression levels of genes related to stemness (**Supplementary Figure 1**). The stimulation of the WNT pathway in BTSCs determined the increased expression of non-phosphorylated (Ser45)  $\beta$ -catenin (active) with respect to total protein amount as demonstrated by WB analysis and by immunofluorescence (**Figure 5B-D**). In turn, the expression of active  $\beta$ -catenin was also increased by stimulating BTSC with Lipopolysaccharides (**Figure 5B-D** and **Supplementary Figure 1**), a substance proved to have proliferative effects on BTSCs(20). The expression of WNT ligands and active  $\beta$ -catenin was further studied *in vivo* in the DDC model. In controls, WNT ligands (Wnt1 and Wnt3a) were rarely expressed by stromal cells within the lamina propria of EHBD (**Figure 5** and **Supplementary Figure 1**). DDC injury increased the percentage of stromal cells expressing WNT ligands around PBGs (p<0.05 versus controls; **Figure 5**). After the recovery period, this significant increase was abolished. In parallel, DDC injury increased active  $\beta$ -catenin expression by PBGs (p<0.05 versus controls) which returned to the level of controls after the recovery period (**Figure 5E**).

Notch pathway activation in human BTSC induces their differentiation to mature cholangiocytes and is associated with PBG activation in DDC-mediated duct injury in mice.

The stimulation of Notch pathway by the administration of recombinant human sDLL-1 determined in BTSCs the increase of Notch intracellular domain (NICD) by WB analysis and NOTCH1 expression by immunofluorescence compared to control conditions (*p*<0.05, **Figure 6A**). The activation of the Notch pathway in BTSCs significantly reduced cell proliferation and stem cell gene expression (**Figure 6B** and

Supplementary Figure 2). Remarkably, The Notch pathway activator specifically triggered cholangiocyte differentiation as showed by i) the up-regulation of mature cholangiocyte genes (i.e. *CFTR*, *SCTR*, *ASBT*) compared to control conditions (Figure 6B), and ii) the expression of mature cholangiocyte marker demonstrated by western blot analysis (i.e. CFTR, AE2, Figure 6C) and by immunofluorescence (i.e. SCTR and presence of primary cilia, Figure 6D). No sign of differentiation towards hepatocyte or endocrine pancreatic lineages was detected when cells were stimulated by the Notch activator (not shown).

The expression of Notch pathway elements was further studied *in vivo* in the DDC mouse model. In controls, Notch1 (**Figure 6E**), Notch2 (**Supplementary Figure 2**), but not Notch3 (**Supplementary Figure 2**) were expressed by few cells within PBGs. DDC injury determined a significant increase of the percentage of PBG cells expressing Notch1, Notch2, and Notch3 compared to controls (p<0.05). After the recovery period, this significant increase was partially reduced, but still higher compared to controls (p<0.05). In parallel, DDC injury increased Jagged1 (a Notch ligand) expression both by PBGs and stromal cells (p<0.05 versus controls), which returned to control levels after the recovery period.

Human Primary Sclerosing Cholangitis is characterized by modification of WNT and Notch pathway expression in PBGs.

In human PSC samples, PBG area was increased compared to control subjects (i.e. liver donors); furthermore, PBGs showed higher percentage of PAS<sup>+</sup> (mucinous), Sox9<sup>+</sup> (stem/progenitor), and PCNA<sup>+</sup> (proliferating) cells compared to controls (**Figure 7A** and **Supplementary Figure 3**).

As regard WNT pathway, the ratio between active β-catenin with respect to total β-catenin expression, quantified in PBGs by an image analysis algorithm, indicated an increased activation of β-catenin in PSC compared to control subjects (**Figure 7B** and **Supplementary Figure 4-5**). Then, to explore *in situ* the possibility that WNT ligands are furnished by inflammatory cells in PSC, we analysed WNT1 and WNT3a given their well-known role in influencing the liver stem cell niche(23). Our results indicated that WNT1 and WNT3a were mostly expressed by inflammatory cells (S100A9<sup>+</sup>) which surrounded PBGs in PSC-affected ducts (**Figure 7C**). As regard Notch pathway (**Figure 7D-F**), PBGs in PSC showed a slight increase in Notch1 expression compared to control samples. Moreover, Notch2 and Hes1 nuclear expression was strongly increased in PSC compared to controls. Interestingly, when Notch ligands were investigated, the expression of DLL4 and Jagged2 was increased in PSC compared to control samples (**Figure 7D-F**). These ligands were expressed by PBG cells, by inflammatory (S100A9<sup>+</sup>) cells, and by stromal (α smooth muscle actin<sup>+</sup>) cells surrounding PBGs.

Given the high expression of WNT and Notch ligands by inflammatory cells in PSC samples, we divided PSC-affected ducts between ducts with high inflammation and ducts with low inflammation (**Figure 8A-C**) based on the presence of more than one inflammatory foci per duct. Interestingly, PSC-affected ducts with high inflammation were characterized by higher PBG mass compared to PSC ducts with low inflammation. In PSC duct with low inflammation, PBGs did not show increased expression of active  $\beta$ -catenin and Notch-1 compared to normal ducts (**Figure 7**). Differently, PBGs within highly inflamed ducts showed an increased active  $\beta$ -catenin and Notch-1 compared to normal ducts with low

inflammation (p< 0.05). Finally, Notch-2 expression by PBGs was significantly increased both in PSC ducts with low and high inflammation compared to control ducts (p< 0.05).

## DISCUSSION

The present study demonstrated that: i) DDC injury in mice mimics typical PSC histopathological lesions, including PBG hyperplasia, mucinous metaplasia and periductal fibrosis; ii) Sox9<sup>+</sup> cells within PBGs proliferate and participate in the regeneration of cholangiocytes lining biliary epithelium after DDC-induced damage; iii) WNT triggers BTSC proliferation and migration while Notch pathway induces their differentiation toward a mature phenotype; iv) in PSC patients, PBG proliferation is associated with sustained activation of WNT and Notch pathways by inflammatory and stromal cells. Altogether, our results support the involvement of BTSCs located in PBGs in the regeneration of the biliary epithelium after injury and in disease progression (**Figure 8D**).

In humans, PBGs represent the niche of BTSCs, a stem/progenitor cell population with multipotent capabilities. Both *in vitro* and *in vivo*, BTSCs can mature towards hepatocyte, cholangiocyte and pancreatic lineages(8, 9). PBGs are not distributed homogeneously along the entire biliary tree; they are present in extrahepatic biliary tree and in larger intrahepatic (i.e. segmental and area) bile ducts(8). The involvement of PBGs and BTSCs in biliary tract pathologies has been described in experimental models(24) and in human cholangiopathies(25). In ischemic biliary lesions, an increased number of proliferating progenitor cells has been demonstrated in PBGs(26); the PBG injury due to ischemia is associated with the occurrence of

biliary strictures after liver transplantation(27). Interestingly, PBGs are also involved in the pathogenesis of biliary strictures in patients with PSC(11, 28); in this disease, chronic biliary inflammation stimulates PBG stem cell niche with subsequent myofibroblast activation, leading to biliary fibrosis and strictures. Furthermore, PBG stem cell niche gives rise to a secondary regenerative response leading to biliary carcinogenesis in human PSC patients(20) and in experimental genetically-induced biliary injury(29). Generally, the emerging concept is that PBG stem cell niche can be activated in the context of pathologies affecting larger IHBDs and EHBDs(8, 30), despite the well-recognized proliferative capability of mature cholangiocytes(4, 31). Thus, the actual contribution of BTSCs in the bile duct regeneration remains an open question.

In this study, biliary injury was experimentally induced in a lineage tracing model. Most of experimental model of biliary injury mainly focused on IHBD and liver fibrosis(32). In contrast, few studies investigated histological damage of extrahepatic ducts and the development of biliary concentric fibrosis (i.e. strictures)(32). Here, we observed that DDC administration was able to induce damage and fibrosis in EHBDs with histological depicts mimicking PSC lesions, including surface epithelium destruction, PBG proliferation and mucinous metaplasia, myofibroblast activation, and concentric fibrosis. Other experimental models have been proved to mimic PSC (e.g. Mdr2 knockout mice)(32); however, the aims of the present study lead to opt for the chemically-induced DDC model instead of genetic ones given the possibility to remove the toxic agent and observe the recovery. Interestingly, DDC administration induced the expansion of the Sox9<sup>+</sup> cell population in PBGs. The Sox9<sup>+</sup> cell compartment extended towards the surface epithelium which became devoid of

AE2<sup>+</sup> and CFTR<sup>+</sup> (i.e. mature) cholangiocytes. The interruption of the DDC diet (recovery period) determined a progressive restoration of the bile duct histology. Our lineage tracing system tracked K19<sup>+</sup> cholangiocytes with an efficiency around 90% in EHBD surface epithelium; following DDC administration, not-tracked cells replenished the surface epithelium, thus indicating a substantial participation of K19<sup>-</sup> cells to the regenerative response. In EHBDs, K19<sup>-</sup> cells were only localized within PBGs and corresponded to the Sox9<sup>+</sup> cell population. In keeping with that, td-Tom<sup>-</sup> cells within surface epithelium of injured ducts were Sox9<sup>+</sup> and CFTR/AE2 negative, thus confirming the PBG compartment as a source of surface epithelial cells in injured ducts. Interestingly, some Sox9<sup>+</sup>/td-Tom<sup>-</sup> cells within surface epithelium showed positivity for K19, indicating sign of initial maturation; this feature was followed by the progressive loss of Sox9 expression and the appearance of functional cholangiocyte markers (i.e. CFTR) during the recovery period. The choice to focus on EHBDs excludes the eventual interference of small Sox9<sup>+</sup> cholangiocytes in our model; small cholangiocytes have proliferative and regenerative capabilities (3, 33); however, this cell compartment is anatomically distinct from the extrahepatic biliary tree since it corresponds to the bile ductules inside the liver parenchyma; moreover, small cholangiocytes express K19, thus phenotypically differing from K19 PBG subpopulation investigated in this study. Taken together, our data indicate an active contribution by Sox9<sup>+</sup> PBG cells in the restoration of surface epithelium after injury and their capability to differentiate into mature cholangiocytes. Our findings are in keeping with the evidence that the regeneration of ischemic injured surface epithelium is ensured by BTSC activation in a human ex vivo model (34).

Stem cell activation is precisely modulated by molecular signals furnished by a specialized niche. In the liver, the hepatic progenitor cell niche is well-characterized and the contribution of Notch and WNT pathways has been thoroughly demonstrated(19, 23). By the contrary, no information is present regarding the signaling pathways which drive BTSC activation. Therefore, the present study further evaluated the activation of WNT and Notch pathways, indicating their role in BTSC proliferation (WNT/β-catenin) or cholangiocyte fate choice (Notch). In DDC, WNT and Notch ligands are furnished by ductal (myo-)fibroblasts around PBGs, thus indicating a putative role of these cells in the niche composition. In this experimental model, further studies based on direct in vivo inhibition/stimulation of signaling pathways would be compelling. However, we pointed our attention on the role of these signals in the contest of human cholangiopathies. Previous studies demonstrated a divergent activation of the PBG niche in PSC compared to primary biliary cholangitis; in primary biliary cholangitis, PBG hyperplasia does not take place since the chronic inflammation primarily involves interlobular bile duct, mostly sparing large intrahepatic and extrahepatic bile ducts(11). Differently, in PSC, PBG niche is activated, especially in ducts with high fibrosis and inflammation(11). The present study further describes a prominent activation of WNT and Notch pathways, potentially supported by ligands from infiltrating inflammatory cells. PBGs can produce themselves Notch ligands, thus suggesting an autocrine effect and a further paracrine effect on neighboring (myo-) fibroblasts. Interestingly, previous evidences indicated that, in human biliary disease, PBGs can secrete vascular endothelial growth factors, influencing the modification of peribiliary vascular plexus in PSC(20) and hypoxic conditions (34, 35). Taken together with previous studies (11, 20), our results indicate that the activation of PBG niche represents a consequence of toxic

or inflammatory biliary damage (**Figure 8**). In the DDC model, Notch and Wnt signalling pathways are turned off once the toxic agent is interrupted, thus determining a progressive restoration to the normal condition. In PSC, chronic inflammation continuously triggers PBG niche activation; in turn, chronically activated PBGs start to produce growth factors (vascular endothelial growth factors)(20, 34, 35), signals (Sonic Hedgehog, Notch Ligands)(11), and inflammatory cytokines (Interleukin-6, Transforming Growth Factor- $\beta$ ), which further stimulate fibrogenetic and inflammatory cells. Therefore, this secretory phenotype(36) of PBGs in PSC configures a sort of vicious circle, which is more prone to developing concentric fibrosis than furnishing coordinated signals for *restitutio ad integrum*. Our results further support the role of PBGs in biliary carcinogenesis in PSC patients; the effects on BTSC proliferation and migration by  $\beta$ -catenin activation and the evidence of prolonged WNT ligand production by chronic inflammation are in touch with the pathogenetic role of WNT pathway in cholangiocarcinoma(37, 38).

In conclusion, the present study furnishes evidence on the direct role of BTSCs in the regeneration of injured biliary epithelium and identified WNT and Notch as key signaling pathways driving BTSC activation, with relevant implications in the pathophysiology and clinical management of cholangiopaties.

#### REFERENCES

- 1. **Cardinale V**, **Wang Y**, Carpino G, Mendel G, Alpini G, Gaudio E, et al. The biliary tree--a reservoir of multipotent stem cells. Nat Rev Gastroenterol Hepatol 2012;9:231-240.
- 2. Han Y, Glaser S, Meng F, Francis H, Marzioni M, McDaniel K, et al. Recent advances in the morphological and functional heterogeneity of the biliary epithelium. Exp Biol Med (Maywood) 2013;238:549-565.
- 3. Glaser SS, Gaudio E, Rao A, Pierce LM, Onori P, Franchitto A, et al. Morphological and functional heterogeneity of the mouse intrahepatic biliary epithelium. Lab Invest 2009;89:456-469.
- 4. Sampaziotis F, Justin AW, Tysoe OC, Sawiak S, Godfrey EM, Upponi SS, et al. Reconstruction of the mouse extrahepatic biliary tree using primary human extrahepatic cholangiocyte organoids. Nat Med 2017;23:954-963.
- 5. Nakanuma Y, Sasaki M, Harada K. Autophagy and senescence in fibrosing cholangiopathies. J Hepatol 2015;62:934-945.
- 6. **Lu WY**, **Bird TG**, Boulter L, Tsuchiya A, Cole AM, Hay T, et al. Hepatic progenitor cells of biliary origin with liver repopulation capacity. Nat Cell Biol 2015;17:971-983.
- 7. Raven A, Lu WY, Man TY, Ferreira-Gonzalez S, O'Duibhir E, Dwyer BJ, et al. Cholangiocytes act as facultative liver stem cells during impaired hepatocyte regeneration. Nature 2017;547:350-354.
- 8. **Carpino G**, **Cardinale V**, Onori P, Franchitto A, Berloco PB, Rossi M, et al. Biliary tree stem/progenitor cells in glands of extrahepatic and intraheptic bile ducts: an anatomical in situ study yielding evidence of maturational lineages. J Anat 2012;220:186-199.

- 9. **Cardinale V**, **Wang Y**, Carpino G, Cui CB, Gatto M, Rossi M, et al. Multipotent stem/progenitor cells in human biliary tree give rise to hepatocytes, cholangiocytes, and pancreatic islets. Hepatology 2011;54:2159-2172.
- 10. **Carpino G**, **Cardinale V**, Gentile R, Onori P, Semeraro R, Franchitto A, et al. Evidence for multipotent endodermal stem/progenitor cell populations in human gallbladder. J Hepatol 2014;60:1194-1202.
- 11. Carpino G, Cardinale V, Renzi A, Hov JR, Berloco PB, Rossi M, et al. Activation of biliary tree stem cells within peribiliary glands in primary sclerosing cholangitis. J Hepatol 2015;63:1220-1228.
- 12. **Carpino G**, **Puca R**, **Cardinale V**, Renzi A, Scafetta G, Nevi L, et al. Peribiliary Glands as a Niche of Extrapancreatic Precursors Yielding Insulin-Producing Cells in Experimental and Human Diabetes. Stem Cells 2016;34:1332-1342.
- 13. **Onori P**, **Alvaro D**, Floreani AR, Mancino MG, Franchitto A, Guido M, et al. Activation of the IGF1 system characterizes cholangiocyte survival during progression of primary biliary cirrhosis. J Histochem Cytochem 2007;55:327-334.
- 14. Carpino G, Renzi A, Cardinale V, Franchitto A, Onori P, Overi D, et al. Progenitor cell niches in the human pancreatic duct system and associated pancreatic duct glands: an anatomical and immunophenotyping study. J Anat 2016;228:474-486.
- 15. **Della Corte C**, **Carpino G**, De Vito R, De Stefanis C, Alisi A, Cianfarani S, et al. Docosahexanoic Acid Plus Vitamin D Treatment Improves Features of NAFLD in Children with Serum Vitamin D Deficiency: Results from a Single Centre Trial. PLoS One 2016;11:e0168216.

- 16. **Nobili V**, **Carpino G**, Alisi A, Franchitto A, Alpini G, De Vito R, et al. Hepatic progenitor cells activation, fibrosis, and adipokines production in pediatric nonalcoholic fatty liver disease. Hepatology 2012;56:2142-2153.
- 17. Nevi L, Cardinale V, Carpino G, Costantini D, Di Matteo S, Cantafora A, et al. Cryopreservation protocol for human biliary tree stem/progenitors, hepatic and pancreatic precursors. Sci Rep 2017;7:6080.
- 18. **Nevi L**, **Carpino G**, Costantini D, Cardinale V, Riccioni O, Di Matteo S, et al. Hyaluronan coating improves liver engraftment of transplanted human biliary tree stem/progenitor cells. Stem Cell Res Ther 2017;8:68.
- 19. Boulter L, Govaere O, Bird TG, Radulescu S, Ramachandran P, Pellicoro A, et al. Macrophage-derived Wnt opposes Notch signaling to specify hepatic progenitor cell fate in chronic liver disease. Nat Med 2012;18:572-579.
- 20. **Carpino G**, **Cardinale V**, Folseraas T, Overi D, Grzyb K, Costantini D, et al. Neoplastic Transformation of the Peribiliary Stem Cell Niche in Cholangiocarcinoma Arisen in Primary Sclerosing Cholangitis. Hepatology 2019;69:622-638.
- 21. Di Matteo S, Nevi L, Costantini D, Overi D, Carpino G, Safarikia S, et al. The FXR agonist obeticholic acid inhibits the cancerogenic potential of human cholangiocarcinoma. PLoS One 2019;14:e0210077.
- 22. Ribaudo R, Gilman M, Kingston RE, Choczynski P, Sacchi N. Preparation of RNA from tissues and cells. Curr Protoc Immunol 2001; Chapter 10:Unit 10 11.
- 23. Boulter L, Lu WY, Forbes SJ. Differentiation of progenitors in the liver: a matter of local choice. J Clin Invest 2013;123:1867-1873.
- 24. **Dipaola F, Shivakumar P**, Pfister J, Walters S, Sabla G, Bezerra JA. Identification of intramural epithelial networks linked to peribiliary glands that express

progenitor cell markers and proliferate after injury in mice. Hepatology 2013;58:1486-1496.

- 25. Zen Y, Liberal R, Nakanuma Y, Heaton N, Portmann B. Possible involvement of CCL1-CCR8 interaction in lymphocytic recruitment in IgG4-related sclerosing cholangitis. J Hepatol 2013;59:1059-1064.
- 26. Sutton ME, op den Dries S, Koster MH, Lisman T, Gouw AS, Porte RJ. Regeneration of human extrahepatic biliary epithelium: the peribiliary glands as progenitor cell compartment. Liver Int 2012;32:554-559.
- 27. op den Dries S, Westerkamp AC, Karimian N, Gouw AS, Bruinsma BG, Markmann JF, et al. Injury to peribiliary glands and vascular plexus before liver transplantation predicts formation of non-anastomotic biliary strictures. J Hepatol 2014;60:1172-1179.
- 28. **Lanzoni G**, **Cardinale V**, Carpino G. The hepatic, biliary, and pancreatic network of stem/progenitor cell niches in humans: A new reference frame for disease and regeneration. Hepatology 2016;64:277-286.
- 29. Nakagawa H, Suzuki N, Hirata Y, Hikiba Y, Hayakawa Y, Kinoshita H, et al. Biliary epithelial injury-induced regenerative response by IL-33 promotes cholangiocarcinogenesis from peribiliary glands. Proc Natl Acad Sci U S A 2017;114:E3806-E3815.
- 30. **Riccio M**, **Carnevale G**, **Cardinale V**, Gibellini L, De Biasi S, Pisciotta A, et al. Fas/Fas ligand apoptosis pathway underlies immunomodulatory properties of Human Biliary Tree Stem/Progenitor Cells. J Hepatol 2014;61:1097-1105.
- 31. Alvaro D, Mancino MG, Glaser S, Gaudio E, Marzioni M, Francis H, et al. Proliferating cholangiocytes: a neuroendocrine compartment in the diseased liver. Gastroenterology 2007;132:415-431.

- 32. **Fickert P**, **Pollheimer MJ**, Beuers U, Lackner C, Hirschfield G, Housset C, et al. Characterization of animal models for primary sclerosing cholangitis (PSC). J Hepatol 2014;60:1290-1303.
- 33. Sato K, Meng F, Giang T, Glaser S, Alpini G. Mechanisms of cholangiocyte responses to injury. Biochim Biophys Acta Mol Basis Dis 2018;1864:1262-1269.
- 34. **de Jong IEM**, **Matton APM**, van Praagh JB, van Haaften WT, Wiersema-Buist J, van Wijk LA, et al. Peribiliary Glands Are Key in Regeneration of the Human Biliary Epithelium After Severe Bile Duct Injury. Hepatology 2019;69:1719-1734.
- 35. Franchitto A, Overi D, Mancinelli R, Mitterhofer AP, Muiesan P, Tinti F, et al. Peribiliary gland damage due to liver transplantation involves peribiliary vascular plexus and vascular endothelial growth factor. Eur J Histochem 2019;63.
- 36. **Tabibian JH**, **O'Hara SP**, Splinter PL, Trussoni CE, LaRusso NF. Cholangiocyte senescence by way of N-ras activation is a characteristic of primary sclerosing cholangitis. Hepatology 2014;59:2263-2275.
- 37. Boulter L, Guest RV, Kendall TJ, Wilson DH, Wojtacha D, Robson AJ, et al. WNT signaling drives cholangiocarcinoma growth and can be pharmacologically inhibited. J Clin Invest 2015;125:1269-1285.
- 38. Guest RV, Boulter L, Dwyer BJ, Kendall TJ, Man TY, Minnis-Lyons SE, et al. Notch3 drives development and progression of cholangiocarcinoma. Proc Natl Acad Sci U S A 2016;113:12250-12255.

Autor names in bold designate shared co-first authorship

#### FIGURE LEGENDS

Figure 1. Biliary damage induces peribiliary gland hyperplasia in rodent extrahepatic bile ducts. A) Hematoxylin & Eosin (H&E) stains on control mice (CTR), in 3,5-Diethoxycarbonyl-1,4-dihydrocollidine (DDC)-fed mice, and 4-week recovery (4-wkREC) mice. DDC-injured ducts showed a marked increase of the wall area fraction occupied by peribiliary glands (PBG, arrows). After the 4-week recovery period, PBG area was reduced compared to DDC mice. B) Periodic Acid-Schiff (PAS) stain on CTR, DDC and 4-wkREC mice. DDC-injured ducts presented a marked increase in the number of PAS<sup>+</sup> cells (arrows) within PBGs, which returned to control value after the recovery period. C) Immunohistochemistry for Proliferating Cell Nuclear Antigen (PCNA) on CTR, DDC and 4-wkREC mice. DDC mice displayed a higher number of PCNA<sup>+</sup> PBG cells (arrows) compared to CTR, which returned to control levels after the recovery period. In histograms, data are reported as means and standard deviation; \*p<0.05 vs all other groups. Scale bars= 100 μm (panels A, B) and 25 μm (C).

Figure 2. Biliary damage induces periductal fibrosis and activation of fibrogenetic cells in rodent extra-hepatic bile ducts. A) Sirius Red (SR) stain in control mice (CTR), in 3,5-Diethoxycarbonyl-1,4-dihydrocollidine (DDC)-fed mice, and 4-week recovery (4-wkREC) mice. DDC administration induced periductal fibrosis with increased wall thickness (inset bars) and higher extent of SR stained fibers compared to CTR. Wall thickness and SR-stained fiber extent were reduced after four weeks of recovery. B) Immunohistochemistry for Collagen I on CTR, DDC and 4-wkREC mice. DDC mice displayed a higher extent of the area fraction occupied by Collagen I fibers compared to CTR. Collagen I fiber extent was reduced

after four weeks of recovery. C) Immunofluorescence for alpha-smooth muscle actin ( $\alpha$ SMA). DDC-injured ducts showed an increase in the number of  $\alpha$ SMA<sup>+</sup> myofibroblasts (green arrows) per high powered field (HPF) within bile duct wall compared to CTR, which returned to control levels after the recovery period. L: bile duct lumen. Green arrowheads indicate smooth muscle cells within artery wall (positive control for  $\alpha$ SMA). Nuclei are displayed in blue. D) Immunofluorescence for desmin. DDC-injured ducts showed an increase in the number of desmin<sup>+</sup> cells (red arrows) per HPF within bile duct wall compared to CTR, which returned to control levels after the recovery period. L: bile duct lumen. Nuclei are displayed in blue. In histograms, data are reported as means and standard deviation; \$p< 0.05 vs all other groups; \*p<0.05 vs control group. Scale bars= 100  $\mu$ m (panels A, C) and 25  $\mu$ m (panels B, D).

Figure 3. Biliary damage in rodent extra-hepatic bile ducts is characterized by the loss of mature cholangiocytes in surface epithelium. A) Double Immunofluorescence for Cytokeratin (K)19 and Sox9 in control mice (CTR) and in 3,5-Diethoxycarbonyl-1,4-dihydrocollidine (DDC)-fed mice. Separate channels are provided. In CTR, virtually all cholangiocytes lining surface epithelium were K19<sup>+</sup>/Sox9<sup>-</sup> (green arrowheads); PBGs were composed of K19+/Sox9+ cells (yellow arrows) and Sox9<sup>+</sup>/K19<sup>-</sup> cells located at the bottom of PBGs (red arrows). In DDC-injured ducts, surface epithelium was characterized by the presence of K19<sup>+</sup>/Sox9<sup>+</sup> cells (yellow arrowheads). Nuclei are displayed in blue. Original Magnification (OM): 40x. B) Double immunofluorescence for Anion Exchanger-2 (AE2) and Cystic fibrosis transmembrane conductance regulator (CFTR) in CTR, and for CFTR and Sox9 in DDC-fed mice. Separate channels are provided. Surface epithelium in CTR ducts

was composed of AE2 and CFTR positive cholangiocytes (yellow arrowheads). Contrarily, in DDC-injured ducts, surface epithelium cells were negative for CFTR but Sox9 positive (red arrowhead). Nuclei are displayed in blue. OM: 40x. C) Immunofluorescence for Sox9 in CTR and DDC mice. In DDC mice, the percentage of Sox9<sup>+</sup> cells increased in PBGs compared to CTR (red arrows). Cells lining surface epithelium (i.e. cholangiocytes) were Sox9<sup>-</sup> in CTR (blue arrowhead) but Sox9<sup>+</sup> in DDC (red arrowhead). Nuclei are displayed in blue. L: bile duct lumen. OM: 10x. The histogram shows mean and standard deviation for the percentage of Sox9<sup>+</sup> cells within PBGs and surface epithelium (SE). \*p<0.05 vs CTR; §p<0.05 vs surface epithelium in CTR; ^p<0.05 vs surface epithelium in DDC.

Figure 4. Peribiliary gland cells participate in the renewal of surface epithelium in injured extrahepatic biliary tree in mice. A) Double immunofluorescence for td-Tomato (td-Tom) and cytokeratin (K)19 in control (CTR), Diethoxycarbonyl-1,4-dihydrocollidine (DDC)-fed, 2-week recovery (2-wkREC), and 4-week recovery (4-wkREC) Krt19CreTdTomatoLSL mice. Separate channels are provided. In CTR mice, most of K19<sup>+</sup> surface epithelial cells (>90%) were lineage tracked and co-expressed td-Tom; only a minority of K19<sup>+</sup> cells was not tracked (green arrow). In DDC-injured ducts, the number of td-Tom- cells within the K19<sup>+</sup> surface epithelium greatly increased (green arrows); in DDC, some tdTom<sup>-</sup>/K19<sup>-</sup> cells were present within surface epithelium (black arrows). During the recovery period, td-Tom<sup>-</sup>/K19<sup>+</sup> cells (green arrows) were present within surface epithelium. Dotted line delimitates bile duct lumen (L). Original Magnification (OM): 20x. B) The histogram shows mean and standard deviation for the percentage of td-Tom<sup>-</sup> cells within surface epithelium (SE). \*p<0.05 vs other groups. C) Double immunofluorescence for td-Tom (in green)

and Sox9 (in red) in DDC mice. Separate channels are provided. In DDC-injured ducts, td-Tom<sup>-</sup>/Sox9<sup>+</sup> were distributed throughout surface epithelium (red arrows). Nuclei (Nu) are displayed in blue. OM: 40x. D) Double immunofluorescence for Cystic fibrosis transmembrane conductance regulator (CFTR) and td-Tom in 4-wkREC mice. Separate channels are provided. Only in 4-wkREC mice, td-Tom<sup>-</sup> cells within surface epithelium showed the appearance of CFTR expression (green arrows). Nuclei are displayed in blue. OM: 40x.

Figure 5. WNT pathway triggers biliary tree stem/progenitor cell activation. A) Proliferation assays in human biliary tree stem/progenitor cells (hBTSCs) cultured in Kubota's Medium (KM), in WNT pathway-stimulation medium (WNT-M), and in WNT-M plus WNT inhibitor (WNT-M+Block). WNT pathway stimulation significantly increased BTSC proliferation as demonstrated by population doubling time (PDT), MTS assay, Cyclin D1 expression by Western Blot (WB) analysis, DNA concentration, and *PCNA* gene expression. The administration of a WNT inhibitor (WNT-M+Block) prevented this effect. B) WB analysis for non-phosphorylated (Nonp)-β-catenin (β-cat) and total β-catenin showed an increased expression of nonphosphorylated (active) form of β-catenin in hBTSCs cultured in WNT-M compared to control conditions (KM). C-D) Immunofluorescence and WB analyses for Non p-βcat expression by hBTSCs cultured in KM, in WNT-M, and in KM + lipopolysaccharides (LPS). Non p-β-cat expression was enhanced in cells under WNT-M and in cells stimulated with LPS (a condition proved to induce BTSC proliferation). Nuclei in panel C are displayed in blue. Original Magnification (OM): 20x. E) Double immunofluorescence for cytokeratin (K)19, Wnt3a (upper panels) and non p-β-cat (lower panels) in controls (CTR), 3,5-Diethoxycarbonyl-1,4-

dihydrocollidine (DDC)-fed mice, and four weeks-recovery (4-wkREC) mice. Compared to controls, DDC-injured ducts displayed an increased expression of Wnt3a (a WNT ligand) in stromal cells (red arrows) around peribiliary glands (PBGs) which declined after the recovery period. In parallel, DDC injury increased non p-β-cat expression by PBGs (yellow arrows), which returned to CTR levels after the recovery period. Nuclei are displayed in blue. Original Magnification: 20x. In panels C and E, the heat maps show semiquantitative (SQ) score of immunohistochemistry or immunofluorescence analyses. In panels A, B and C, data in histograms represent means and standard deviation. \*p<0.05 vs controls; °p<0.05 vs other groups. GOI: Gene of Interest

Figure 6. Notch pathway drives maturation of biliary tree stem/progenitor cells into cholangiocyte. A) Western blot (WB) analysis for Notch Intracellular Domain (NICD) and immunofluorescence for Notch1 in human biliary tree stem/progenitor cells (hBTSC) cultured in Kubota's Medium (KM) and under Notch pathwaystimulation medium (Notch-M). WB and immunofluorescence analyses showed an increased expression of NICD and Nocth1 in hBTSCs cultured in Notch-M compared to control conditions (KM). Nuclei are displayed in blue. Original Magnification (OM): 20x. B) PCR analysis for *PCNA* gene and for genes related to cholangiocyte differentiation in KM and in Notch-M. The activation of Notch pathway in hBTSCs significantly decreased the proliferation marker *PCNA* compared to control conditions (KM). Notch pathway activation significantly increased the expression of mature cholangiocyte genes (i.e. *SCTR*, *CFTR* and *ASBT*) in BTSCs compared to control conditions (KM). Data are expressed as means and standard deviation.

in BTSC stimulated with Notch activator (Notch-M) compared to control condition (KM). Data are expressed as means and standard deviation. \*p<0.01 vs KM. D) Immunofluorescence for Secretin Receptor (SCTR) and α-tubulin in hBTSCs cultured in KM and in Notch-M. The stimulation of Notch pathway induced the expression of the mature cholangiocyte marker SCTR and increased the number of cells displaying a primary cilium (green arrows), compared to self-replication conditions (KM). Nuclei are displayed in blue. OM: 20x (left) and 40x (right). E) Double immunofluorescence for cytokeratin (K)19 and Notch1 (upper panels), and for α smooth muscle actin (αSMA) and Jagged (Jag)1 (lower panels) in control mice (CTR), 3,5-Diethoxycarbonyl-1,4-dihydrocollidine (DDC)-fed mice, and four weeksrecovery (4-wkREC) mice. DDC-injured ducts displayed higher cytoplasmic and nuclear (arrows) expression of Notch1 in peribiliary glands (PBGs) compared to controls; Notch1 expression is partially reduced after 4-week recovery period. In parallel, DDC injury increased Jag1 (a Notch ligand) expression both by PBGs (arrows) and stromal cells (arrowheads), which returned to control levels after the recovery period. Nuclei are displayed in blue. OM: 20x. The heat map reports the semiquantitative (SQ) score of immunofluorescence analyses in CTR, DDC and 4wkREC mice.

Figure 7. WNT and Notch pathways in primary sclerosing cholangitis. A)

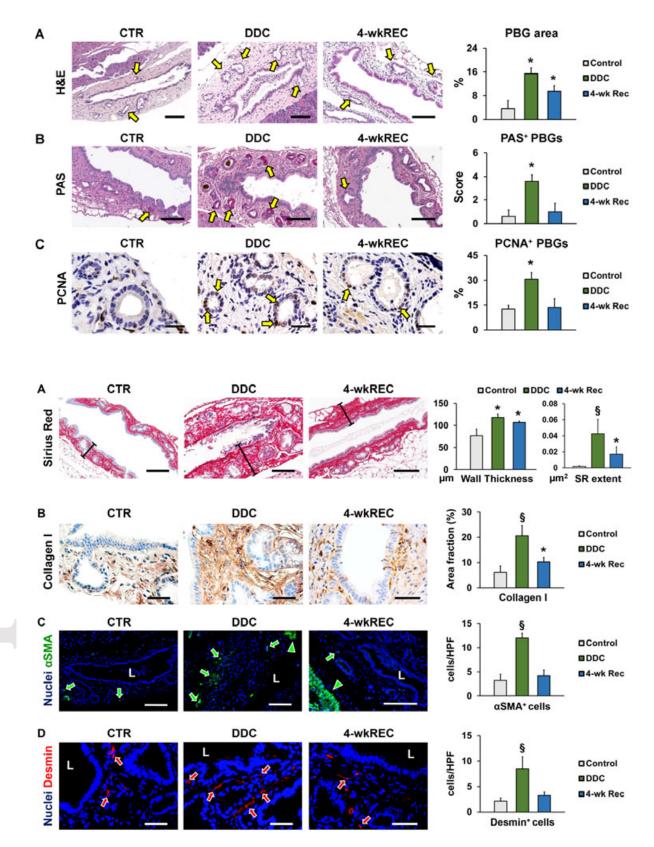
Immunohistochemistry for cytokeratin (K)7 (upper panels) and for proliferating cell nuclear antigen (PCNA, lower panels) in human normal bile ducts and in primary sclerosing cholangitis (PSC)-affected ducts. K7 images showed an increased peribiliary gland (PBG) mass in PSC samples compared to normal ones. Original Magnification (OM): 20x. PBGs in PSC displayed higher expression of PCNA

(arrows) compared to controls. OM: 40x. B) Image analysis algorithm output of immunohistochemistry for non-phosphorylated (Non p-) β-catenin (β-cat) and total βcat on normal and PSC-affected ducts; yellow, orange, and red colours indicate weak, intermediate and strong positivity, as assessed by an image analysis software. The ratio between non p- $\beta$ -cat and total  $\beta$ -cat expression indicated an increased activation of β-cat in PSC samples compared to control subjects. OM: 20x. C) Double immunofluorescence for S100A9 and Wnt1 (panels on the left), and for S100A9 and Wnt3a (panels on the right) in PSC-affected ducts. In PSC-affected ducts, Wnt1 and Wnt3a were mostly expressed by inflammatory (S100A9+) cells (arrows) infiltrating bile ducts and located around PBGs. Separate channels are provided. OM: 40x. D) Immunohistochemistry for Notch1, Notch2, and Hes1 in human normal bile ducts and PSC-affected ducts. PBGs in PSC showed a slight increase of Notch1 nuclear expression (arrows) but strong increase of Notch2 and Hes1 nuclear expression (arrows) compared to normal samples. OM: 40x. E) In upper images, immunofluorescence for Jagged (Jag)2 and for Delta Like Ligand (DLL) 4 in human PSC-affected ducts is reported. PBGs (white asterisks) in PSC showed expression of Notch ligands (arrows). DLL4 is also expressed by stroma cells (arrowhead) around PBGs. OM: 40x. Images in the middle represent double immunofluorescence for α Smooth Muscle Actin (αSMA) and Jag2 in PSC-affected ducts. αSMA<sup>+</sup> myofibroblasts (arrowheads) and PBGs (arrows) in PSC expressed Jag2. In lower images, double immunofluorescence for S100A9 and DLL4 in PSCaffected ducts is displayed. S100A9<sup>+</sup> inflammatory cells around PBGs expressed DLL4 (arrowheads). Separate channels are provided. OM: 40x. F) Heat map visualizing semiguantitative (SQ) score of immunohistochemical and immunofluorescence analyses in human normal ducts and PSC-affected ducts. In

immunofluorescence images, white asterisks individuate PBGs and nuclei are displayed in blue.

Figure 8. WNT and Notch pathways in primary sclerosing cholangitis. A) Sirius Red (SR) stains (upper panels) and immunohistochemistry for cytokeratin (K)7 (lower panels) in primary sclerosing cholangitis (PSC)-affected bile ducts. PSC ducts with high inflammation were characterized by higher peribiliary gland (PBG) mass compared to PSC ducts with low inflammation (arrows). Asterisks individuate inflammatory foci. Original Magnification (OM): 10x B) Immunohistochemistry for non-phosphorylated (non p-) β-catenin, Notch1, and Notch2 in PSC-affected ducts. PBGs within highly-inflamed ducts showed increase in non p-β-catenin and Notch-1 compared to PSC ducts with low inflammation. Notch-2 was strongly expressed by PBGs both in PSC ducts with low and high inflammation. Arrows point positive PBGs. OM: 40x. C) The heat map shows semiquantitative (SQ) scores of immunohistochemical analyses in examined PSC-affected ducts. D) Graphical abstract of main results obtained in the present study. *In vivo*, the Sox9<sup>+</sup> PBG cell population participates to surface epithelial (SE) regeneration in damaged ducts by generation of cells with mature cholangiocyte traits. The contribution of PBG cells in this model is driven by WNT and Notch pathway activation. In vitro, WNT and Notch pathways can induce, respectively, proliferation/migration and cholangiocyte differentiation in Biliary Tree Stem Cells (BTSC). In human PSC, biliary strictures are due to bile duct wall fibrosis. This and previous studies indicated that WNT and Notch pathways have a putative role in the vicious circle at the basis of bile duct fibrosis by mutual influencing PBGs, inflammatory cells, myofibroblasts and microvessels. SHH: Sonic Hedgehog, IL-6: interleukin-6, TGF-β: Transforming

Growth Factor  $\beta$ , VEGFs: Vascular Endothelial Growth Factors; DDC: 3,5-Diethoxycarbonyl-1,4-dihydrocollidine.



С

Nuclei Sox9

